International Journal of Heat and Mass Transfer 52 (2009) 309–315

Contents lists available at ScienceDirect

International Journal of Heat and Mass Transfer

journal homepage: www.elsevier.com/locate/ijhmt

Sublimation rate and the mass-transfer coefficient for snow sublimation

Thomas A. Neumann [a,*], Mary R. Albert [b], Chandler Engel [a,c], Zoe Courville [b], Frank Perron [b]

[a] Department of Geology, University of Vermont, Burlington, VT 05405, USA
[b] U.S. Army Corps of Engineers Cold Regions Research and Engineering Laboratory, Hanover, NH 03755, USA
[c] Department of Civil, Environmental, and Architectural Engineering, University of Colorado, Boulder, CO 80309, USA

ARTICLE INFO

Article history:
Received 24 September 2007
Received in revised form 25 April 2008
Available online 18 July 2008

Keywords:
Sublimation
Snow
Mass transfer
Mass-transfer coefficient

ABSTRACT

Sublimation of snow is a fundamental process that affects the crystal structure of snow, and is important for ice core interpretation, remote sensing, snow hydrology and chemical processes in snow. Prior investigations have inferred the sublimation rate from energy, isotopic, or mass-balance calculations using field data. Consequently, these studies were unable to control many of the environmental parameters which determine sublimation rate (e.g. temperature, relative humidity, snow microstructure). We present sublimation rate measurements on snow samples in the laboratory, where we have controlled many of these parameters simultaneously. Results show that the air stream exiting the snow sample is typically saturated under a wide range of sample temperature and air-flow rate, within measurement precision. This result supports theoretical work on single ice grains which found that there is no energy barrier to be overcome during sublimation, and suggests that snow sublimation is limited by vapor diffusion into pore spaces, rather than sublimation at crystal faces. Undersaturation may be possible in large pore spaces (i.e. surface- or depth-hoar layers) with relatively high air-flow rates. We use these data to place bounds on the mass-transfer coefficient for snow as a linear function of Reynolds number, and find that $h_m = 0.566\ Re + 0.075$.

1. Introduction

The sublimation of ice or snow is driven by an imbalance between the saturation vapor pressure (or vapor density) at a given temperature, and the vapor pressure in the immediate vicinity of an ice surface. If the former exceeds the latter, ice or snow sublimates to eliminate the imbalance. The sublimation rate of ice or snow has important implications for surface energy balance calculations [1], mass balance calculations [2], studies of stable isotope ratios [3], and studies of snow metamorphism [4]. Most prior work has assumed that pore spaces within snow or firn (snow more than one year old) are always at the saturation point [5], obviating the need for an explicit calculation of the sublimation rate within snow.

Although vapor movement through variably saturated firn due to diffusion and ventilation has been modeled [6], because of a lack of laboratory data the mass-transfer coefficient governing sublimation had to be estimated. Prior work on determining the sublimation rate of snow or ice in the laboratory has typically focused on sublimation of single ice particles during forced convection under high flow rates [7,8], while field work has typically used meteorological observations to infer sublimation rate from energy balance considerations [1].

In the present study, we attempt to directly measure the sublimation rate of a snow sample under forced convection in the laboratory. This setting allows us to control many of the parameters that influence sublimation rate in nature (i.e. grain size, microstructure, temperature, air flow through snow (referred to as 'ventilation'), and impurity content). Our methodology relies on precise measurement of the vapor density of an air stream prior to, and after passing through a snow sample of sieved snow grains with coincident measurements of the sample temperature and air-flow rate. We use our data to generate a revised estimate of the mass-transfer coefficient for snow sublimation as a function of Reynolds number. We discuss our results in terms of the physics of sublimating ice grains and compare our results with other models used to calculate snow sublimation rate.

2. Methods

Our approach is to induce air flow through a snow sample in a sealed chamber at a specified temperature and measure the change in relative humidity (via a chilled-mirror hygrometer, which measures the frost point) as the air passes through the sample. We measure the snow sample temperature, the vapor density, ρ, of the air stream both up- and down-stream of the sample, the

* Corresponding author. Tel.: +1 802 656 0687; fax: +1 802 656 0045.
E-mail address: Thomas.Neumann@uvm.edu (T.A. Neumann).

0017-9310/$ - see front matter © 2008 Elsevier Ltd. All rights reserved.
doi:10.1016/j.ijheatmasstransfer.2008.06.003

Nomenclature

a_s	specific surface area of snow (m^{-1})
d_p	grain diameter (m)
D	diffusivity of water vapor in air ($m^2\ s^{-1}$)
h_m	mass-transfer coefficient ($m\ s^{-1}$)
K	thermal conductivity of air ($W\ m^{-1}\ K^{-1}$)
L_s	latent heat of sublimation ($J\ kg^{-1}$)
m	mass (kg)
M	molar mass of water ($kg\ mol^{-1}$)
Nu	Nusselt number (dimensionless)
Pr	Prandtl number (dimensionless)
r	grain radius (m)
R	gas constant ($J\ K^{-1}\ mol^{-1}$)
Re	Reynolds number (dimensionless)
S	sublimation rate ($kg\ s^{-1}$)
Sc	Schmidt number (dimensionless)
Sh	Sherwood number (dimensionless)
T	temperature (K)
v	air flow velocity ($m\ s^{-1}$)
V	volume (m^3)

Greek symbols

ν	kinematic viscosity ($m^2\ s^{-1}$)
ρ	vapor density ($kg\ m^{-3}$)
σ	degree of undersaturation (dimensionless)
ϕ	porosity (dimensionless)

Subscripts

a	air
in	incoming
out	outgoing
sat	saturation

temperature and flow rate of the air stream, and the pressure drop across the sample. A schematic of the apparatus is shown in Fig. 1.

We use sieved aged natural snow composed of a specified grain size (0.85 mm < grain diameter < 2.00 mm) to form disc-shaped snow samples of radius 7 cm and thickness between 1 and 5 cm. The snow sample is sifted into a ring of clear PVC, with fittings to allow thermocouple wire to be incorporated into the sample as it is formed. The sample is then clamped between two 30 cm long chambers with smaller radii (5.25 cm); foam gaskets (5 mm thick) are used between the snow sample and the chamber to prevent air exchange between the sample chamber and the surrounding air. The larger diameter of the snow sample prevents air flow from being channeled between the snow sample and the ring holding the sample. The sample chambers on either side allow the flow to expand from small-diameter tubing (0.635 cm flexible Tygon), which connects the sample chamber to the air stream, to the larger diameter of the snow sample. The entire sample chamber is housed in an insulated box connected to a re-circulating bath which keeps the snow sample and air stream at a constant and uniform temperature.

Upstream of the sample chamber, the forced flow of dry air ($\rho = 0\ kg\ m^{-3}$) is controlled with a needle valve and flow rate is recorded (Sierra Instruments model 720 flow meter). The desired water vapor density is introduced to this air stream via a saturator, constructed following the method of Morris [9]. Our saturator is ~3 m of coiled copper tubing inserted in a re-circulating bath. Dry air is bubbled through a tank of water at 25 °C, and then forced through the saturator (set to −25 °C) at a high flow rate (~20 liters per minute (LPM)). Frost is deposited on the copper coils for 30 min as the air cools and water vapor condenses; air exits at the saturation vapor density ($\rho = \rho_{sat}$) determined by the bath temperature. After frost deposition, air with any ρ can be generated by passing dry air through the saturator, after setting the bath temperature appropriately. This method is capable of generating an air stream with a constant ρ to within our measurement precision of the frost point (±0.2 °C) for several hours at a low flow rate before the frost layer is exhausted.

After passing through the saturator, the air stream is directed into a collapsible ~1 L reservoir with an exhaust port. Air is drawn via vacuum from this reservoir, sequentially through a chilled-mirror hygrometer (General Eastern model 1211H; [10]), the sample chamber containing the snow sample, a second hygrometer (General Eastern model 1211H), a second air flow meter (Sierra Instruments model 822S), a needle valve to control vacuum strength, and finally through a vacuum pump. The collapsible reservoir acts as the source for air drawn through the sample; as long as the flow rate into the reservoir is larger than the flow out of the reservoir, the air drawn through the snow sample has a known source and water vapor content. We also experimented with pushing air through the snow sample, but found that even at the low flow rates considered here (<10 LPM), this led to flow channelization through the center of the snow sample, as evidenced by the evolution of a conical-shaped region of sublimation on the upwind face of the snow sample. Drawing air through the snow sample via a vacuum pump generates near-parallel flow through the snow sample, as evidenced by the even retreat of the upwind face of the sample during sublimation.

3. Results

We sifted snow to select grains between 0.85 and 2.00 mm in diameter to form disc-shaped snow samples with thicknesses of

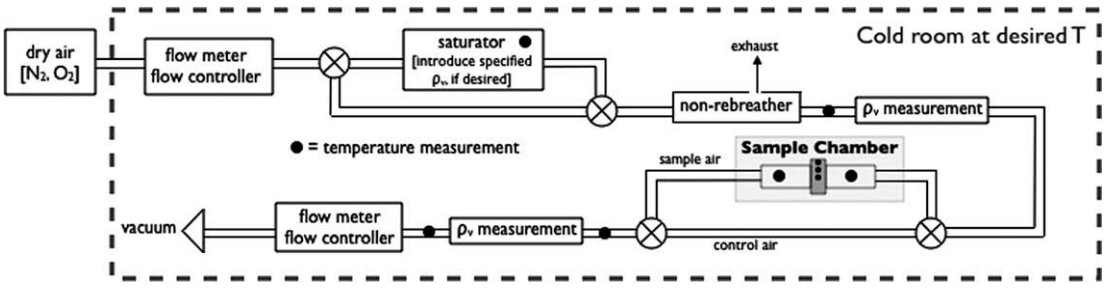

Fig. 1. Diagram of apparatus used for our experiments. Air is drawn through the sample via a vacuum at the lower left. The cold room is maintained at a constant temperature to within ~1 °C; a re-circulating bath maintains a constant temperature in the sample chamber to within 0.1 °C.

5, 2.5 and 1 cm. We measured the snow sublimation rate of these samples in 34 different simulations using a range of sample temperature (−5, −9, −13, −19 and −23 °C) and air-flow rate (between 1 and 10 LPM). These flow rates correspond to residence times of air in the snow sample of between 26 and 0.5 s, depending on the particular snow sample thickness and air-flow rate being considered. These temperatures and flow rates were selected to approximate the temperature and air-flow rates due to firn ventilation experienced by near-surface polar snow [6].

Although the re-circulating bath keeps the inlet air stream and the sample chamber at a constant and uniform temperature, the snow sample cooled during tests due to the latent heat loss during sublimation. Fig. 2 shows the typical temperature change during a test. In this plot, the three bold curves correspond to temperature measurements from three different thermocouple probes embedded in the snow sample. These thermocouples were placed in the same plane in the sample, equidistant from the front and rear faces of the sample. Thermocouple A (bold solid curve) was placed at the center of the snow sample (7 cm from sample edge), thermocouple B (bold dashed curve) was placed midway between the center and the edge of the sample (3.5 cm from sample edge), and thermocouple C (bold dotted curve) was placed 1 cm from the edge of the sample; this is within the overlap resulting from the differing diameters of the sample and the air-flow chamber. Consequently, we expect little or no air flow through the sample at probe C. The two thin curves correspond to measurements of the air temperature upstream (thin solid curve) and downstream (thin dashed curve) of the snow sample. In this test, the air-flow rate was 5 LPM, and the flow began at time = 0 h.

This figure shows that probes A and B experienced approximately the same cooling throughout the test (∼1 °C), but that probe C cools appreciably slower, suggesting that sublimation was much slower when the air flow velocity (v) is significantly reduced as in the overlap area, as expected. After the first 30 min, probes A, B and C cooled much more slowly, reflecting the influence of conduction from the warmer sample chamber and re-circulating bath. In very long duration tests (not shown), the sample eventually developed a constant, heterogeneous temperature distribution that was coldest at the center and warmest at the edges; the magnitude of the difference was a function of the snow structure (i.e. the effective thermal conductivity), sublimation rate and sample chamber temperature. In Fig. 2, the influence of conduction from the re-circulating bath is apparent, as the sample temperature relaxes exponentially back to the initial temperature after air flow (and consequently, sublimation) ceases at time ∼3.1 h. The two air-temperature probes (thin curves) were located in the entrance and exit chambers ∼10 cm from the snow sample, and show relatively little temperature change, although a slight cooling of the air temperature downstream of the sample is evident.

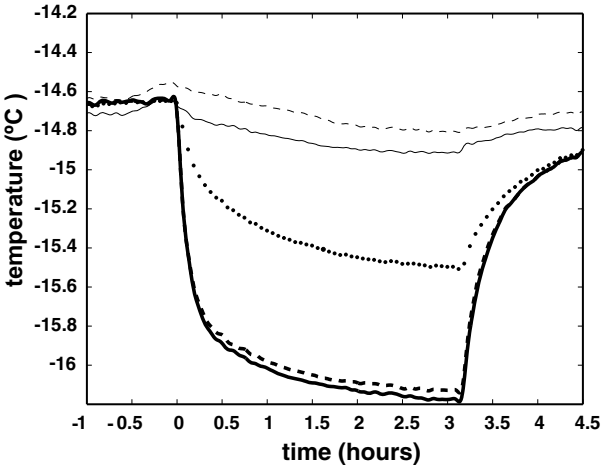

Fig. 2. Plot of temperature change from typical run: $T = -15$ °C, flow rate = 5 LPM, sample thickness = 2.5 cm. Thick solid curve = temperature at sample center (7 cm from edge), thick dashed curve = temperature 3.5 cm from edge, and thick dotted curve = temperature 1 cm from edge, thin solid curve = temperature of air entering the sample chamber, thin dashed curve = temperature of air leaving sample chamber.

Ideally, the sublimation rate of the sample can be controlled by varying the vapor density of the air entering the sample chamber (ρ_{in}) using the saturator and by varying the air-flow rate and the temperature in the chamber. Our goal in this work was to bracket the range of possible sublimation rate for a given temperature and flow rate; consequently, we used dry air (frost point $T < -50$ °C, or $\rho < 3.8 \times 10^{-5}$ kg m^{-3}; [11]) to produce the results presented here.

Our sublimation rate measurements are presented in Fig. 3 as a function of flow rate. We calculate the sublimation rate (kg s^{-1}) during a given run by converting the frost point data from the downstream sensor (°C) to vapor pressure (Pa) and then to vapor density (kg m^{-3}). The sublimation rate is found by multiplying the vapor density by the air-flow rate (measured as a volumetric air flux, m^3 s^{-1}). We calculate the sublimation rate from each pair of frost point and flow meter data (collected every 2 s) during the run, and then average over the duration of the run to generate a single sublimation rate. These data are indicated by the open circles in Fig. 3. The vertical bars on each circle denote the standard deviation of the high-frequency sublimation rate data, and are a measure of the uncertainty in our inferred sublimation rate. This uncertainty is primarily due to uncertainty in the frost point measurement (±0.2 °C). A second, much smaller, source of uncertainty is due to uncertainty in the flow meter data. In Fig. 3, each panel corresponds to the approximate sample temperature during the series of runs (i.e. $T = -5$, −10, −15, −20 and −25 °C).

Most of the data presented in Fig. 3 used 2.5 cm thick samples; half of the runs at −20 °C and all of the runs at −25 °C used 1 cm thick samples. The difference in calculated sublimation rate at a given temperature for samples with different thicknesses is indistinguishable on the scale of Fig. 3. That is, according to our results, sample thickness (and hence residence time) does not contribute significantly to the calculated sublimation rate. We discuss this further below.

The open triangles in Fig. 3 represent the theoretical maximum sublimation rate possible for each run. The theoretical maximum sublimation rate is calculated using the mean air temperature downstream of the snow sample and mean flow rate during the run and by assuming that $\rho_{in} = 0$, and that $\rho_{out} = \rho_{sat}$, where $\rho_{sat}(T)$ is given by the Clausis–Clapeyron relation with respect to ice. It is evident that, regardless of flow rate, sample thickness and temperature, our measured sublimation rates are very close to the theoretical maximum.

A second way to present our data is to compare our measured sublimation rate with our estimate of the maximum sublimation rate as a percentage. The data from all tests are binned into intervals of 2% in Fig. 4. This analysis shows that 74% (25 of 34) of our measurements lie within 5% of the theoretical maximum value, regardless of temperature, flow rate, or sample thickness.

4. Discussion

Our data (e.g. Fig. 4) suggest that the snow sublimates rapidly, and that for snow samples with thickness 1 cm or greater, pore spaces in snow are typically saturated with vapor, as other investigators have assumed [5]. The largest uncertainty in our measurements is due to the frost-point hygrometers (±0.2 °C), followed by uncertainty in the flow meter data. A tertiary source of uncertainty

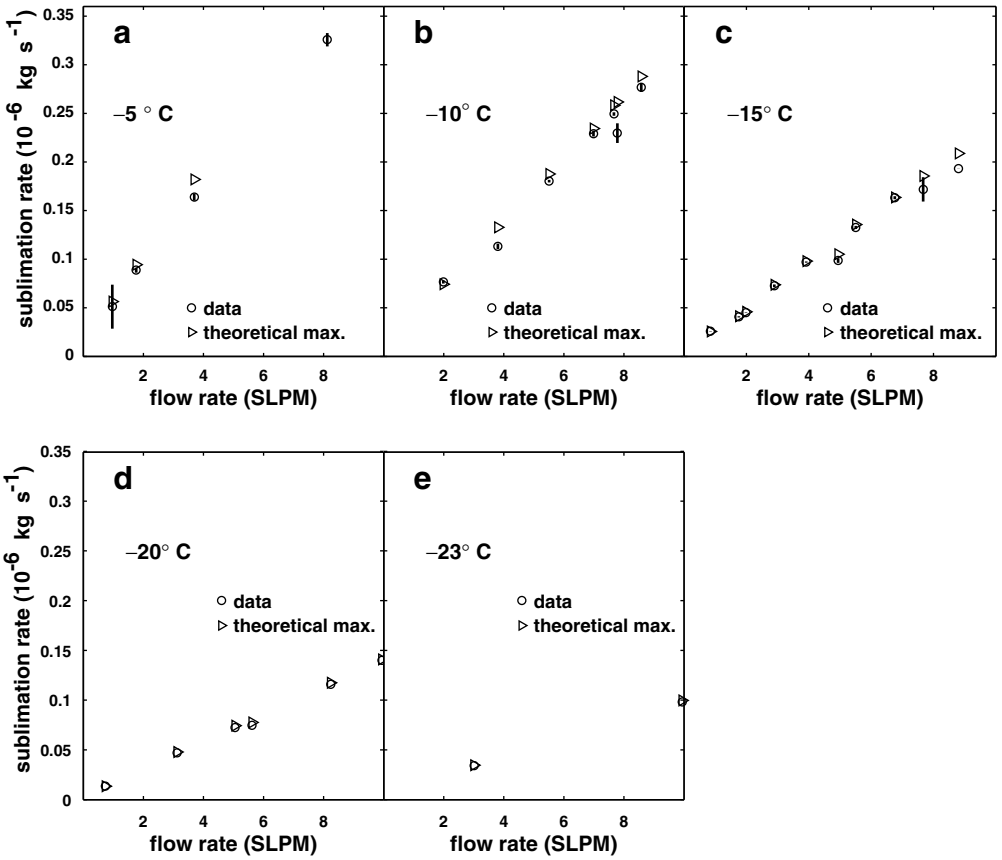

Fig. 3. Plot of sublimation rate as a function of flow rate, for five different temperature ranges. Open circles are data, open triangles correspond to theoretical maximum sublimation rate at the same temperature and flow rate used in each run.

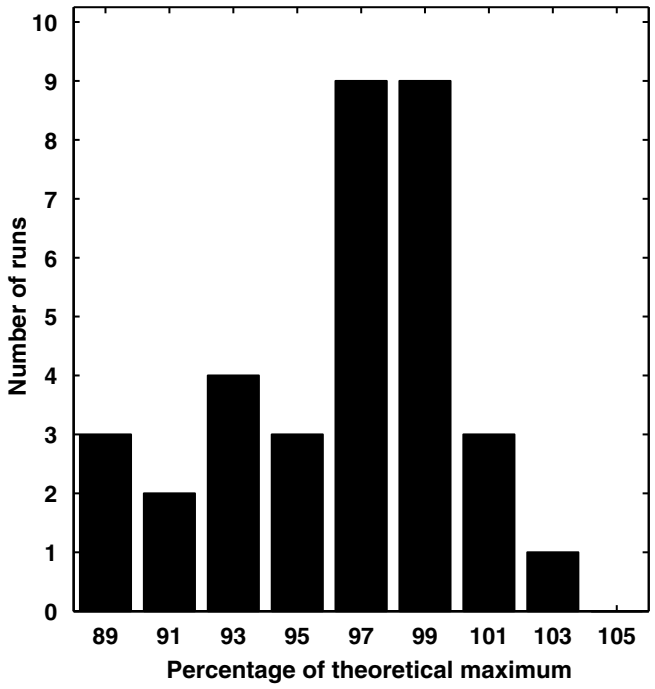

Fig. 4. Histogram of data, plotted as percentage of theoretical maximum sublimation rate, binned in 2% intervals.

is how best to deal with the changing, non-uniform snow sample temperature (Fig. 2). To generate the results presented in Figs. 3 and 4, we calculate the theoretical maximum sublimation rate for a given test as a function of time, using the thermocouple data from the air downstream of the snow sample, as described above. We assume that this temperature is representative of the air temperature in the snow sample pore space. Ideally, we would calculate the distribution of ρ_{sat} for a given air temperature distribution in the snow sample. It is evident in Fig. 4 that the inferred sublimation rates of most of the runs (25 of 34) lie within 5% of being perfectly saturated. The remaining runs show some degree of sub-saturation of the air stream leaving the snow sample. Intuitively, one might expect that tests with either large flow rates, or small sample thickness, or both, would produce sub-saturated air leaving the snow sample. The lowest saturation ratios (85%, 86% and 89% of maximum possible rate) are collected into the 89% bin, and represent tests on 2.5 cm thick samples at flow rates of 8, 4 and 8 LPM flow rates, supporting this hypothesis. However, of the 14 tests conducted at flow rate greater than 5 LPM, 9 of them are within 5% of saturation. Furthermore, of the 9 tests below 95% saturation, 4 of them have flow rates of 5 LPM or smaller. So while these results qualitatively suggest that higher air flow rates correspond to lower saturation of the airstream leaving the snow sample, the results are not conclusive; better representation of the pore space air temperature and the non-uniform sublimation rate in the sample (as indicated by sample temperature data in Fig. 2) could help clarify this issue. For our purposes, we conclude that air leaving the snow sample is usually saturated, although some evidence for sub-saturation exists.

Recent work on the growth and melt of single crystals suspended in liquid by Cahoon et al. [12] provides insight into the micro-scale processes active during mass transfer from crystals to the environment. The experimental and theoretical results of Cahoon et al. [12] demonstrate that there is no energy barrier to be

overcome during the addition or removal of material at the molecularly rough corners of the classic faceted snow crystal with six-fold symmetry. During both grain growth and melt, the addition or removal of material at these rough edges is much faster than on faceted surfaces, where the exchange of material is an activated process. This lack of an energy barrier causes the activity at the rough edges to dominate the morphology of ice crystals, and may explain our rapid sublimation rates.

If this conceptual picture is appropriate for sublimation of crystals as well as for the melt forms investigated by Cahoon et al. [12], then transfer of heat toward and water vapor away from the sublimating interface may limit the sublimation rate of a polycrystalline aggregate. Ice crystals sublimate as dry air enters the snow sample; water vapor is advected throughout the pore space by air flow until saturation vapor pressure is reached, preventing further sublimation. In an adiabatic system, the crystal surface would also continue to cool due to latent heat loss, until the ice surface temperature and vapor density reached an equilibrium dictated by the Clausis–Clapeyron relation. The two processes that promote continued sublimation are advection or diffusion of water vapor away from the ice-air interface (diffusivity of water vapor in air $\sim 2 \times 10^{-5}$ m^2/s) and the diffusion of heat through the ice crystal (thermal diffusivity in ice $\sim 1 \times 10^{-6}$ m^2/s). Sample temperature data (Fig. 2) demonstrate that the sample cools for the first $\sim$15 min after sublimation begins. After that time, heat conduction through the crystal structure in the rest of the snow sample and sample chamber (kept at a constant temperature by the re-circulating bath) buffer further temperature change. Ultimately, equilibrium is reached between cooling due to the latent heat of sublimation for a given flow rate and heat exchange with the sample chamber. Our results show that sublimation rates are small and that saturation vapor density is reached before the sample cools by more than a few °C. In this model, sublimation of snow at the microscopic level is then essentially instantaneous; the bulk sublimation rate is limited by the air-flow rate (i.e. firn ventilation) and the sample temperature.

We can assess this model by comparing the characteristic times for advection and diffusion in our experiments. Our sieved snow samples have pore space volume on the order of 1 mm^3. Using the diffusivity of water vapor in air of Massman [13], the diffusion timescale from the surface of an ice grain to the center of the pore space is $\sim$0.05 s. With the highest flow rate (Darcy velocity = 1.9 cm s^{-1}), the residence time of air in the 1 cm thick snow sample is much longer ($\sim$0.5 s); the residence time of air in a single pore space (using pore velocity) is $\sim$0.02 s. These characteristic times suggest that ρ_{sat} should be reached in the first few mm of the snow sample, providing support for the Cahoon et al. [12] model. In this case, pore spaces in snow or firn reach saturation vapor density in the first layer or two of snow grains and are virtually always saturated. It may be possible to temporarily generate undersaturated air in either large pore spaces (>1 cm or larger) or with rapid air flow through snow packs or firn (>5 cm s^{-1}).

In our experiments, the saturation vapor density is reached in the first few mm and that the air leaving the snow sample is typically saturated, regardless of the sample thickness used. The sublimation rate should be independent of sample thickness (or residence time) unless the sample thickness is less than or equal to the depth in the sample where saturation is achieved; or equivalently, unless the residence time is less than that required for saturation to be reached. Consequently, we have plotted the sublimation rate as a function of flow rate, rather than residence time, in Fig. 3 to highlight the relationship between the sublimation rate and the air-flow rate.

The work of Thorpe and Mason [7] provides another means of evaluating our inferred sublimation rates. They measured and modeled the sublimation of isolated ice spheres in a stream of air of known humidity with relatively rapid flow rates ($Re > 10$). A similar approach [8] was used to model the sublimation of ice cylinders, though at much more rapid flow ($950 < Re < 9000$). Other investigators used the model of Thorpe and Mason [7] to study the sublimation of blowing and saltating snow grains [14]. In this model, the mass rate of change, dm/dt, of an ice grain is given by

$$\frac{dm}{dt} = \frac{2\pi r \sigma}{\frac{L_s}{KTNu}\left(\frac{L_s M}{RT} - 1\right) + \frac{1}{DSh\rho_{sat}(T)}} \quad (1)$$

where r = grain radius, σ = degree of undersaturation (= 0 for fully saturated air), L_s = latent heat of sublimation, K = thermal conductivity of air, T = ice grain temperature, Nu is the Nusselt number, M is the molar mass of water, R is the gas constant, D is the diffusivity of water vapor in air, $\rho_{sat}(T)$ is the saturation vapor density at T, and Sh is the Sherwood number. The Reynolds number for our experiments ($0.25 < Re < 3.5$) is lower than that studied by Thorpe and Mason [7], but further work [14] suggests this relation may be appropriate at lower Re. In this work, we have assumed that:

$$Nu = 1.88 + 0.66 Pr^{0.333} Re^{0.5} \quad (2)$$

$$Sh = 1.88 + 0.66 Sc^{0.333} Re^{0.5} \quad (3)$$

where Pr is the Prandtl number (= kinematic viscosity of air (ν_a)/thermal diffusivity of air) and Sc is the Schmidt number (= ν_a/diffusivity of water vapor in air). This model suggests that ρ_{sat} should be reached in the first few mm of the sample for all of our experiments, which is consistent with our results. We scale the results of Eq. (1) for a single sublimating grain to our aggregate measurements using estimates for the number of grains in the first few mm of our sample. Assuming that the above relation holds for only the first layer of ice grains (grain diameter $\sim$1.3 mm) in the sample, and that all grains in this layer sublimate at the same rate, Eq. (1) predicts sublimation rates approximately a factor of 4 faster than our measurements. This result suggests that either all grains in the first layer do not sublimate at the same rate, our estimate for the number of grains in the actively sublimating region is too large, or that we have not adequately accounted for the contact area between grains. In any case, we conclude that saturation vapor density is reached between 2 mm and 1 cm depth (i.e. between the first layer of snow grains and the entire thickness) in the snow sample.

Using the temperature data (e.g. Fig. 2) and the measured sublimation rate, we can determine to what extent our experiment conserves energy. If the experiment is adiabatic, in a given time period, the difference between the sensible heat carried into and out of the sample by air flow should be balanced by the internal energy change of snow sample and the energy used for sublimation. In our experiment the energy balance is dominated by the latent heat of sublimation, and that these terms are never perfectly in balance, summing to between -10 and -40 J min^{-1}. If all of this energy is used to cool the snow sample, the sample temperature would decrease by an additional $\sim$0.1 K min^{-1}, well above our detection limit. This residual energy can be expressed as a linear function of the flow rate ($r^2 = 0.72$). This is not surprising, given the linear relationship between sublimation rate and Reynolds number (discussed below). We suggest that this energy imbalance is due to either energy exchange with the air stream, surrounding apparatus (i.e. sample chamber, re-circulating bath) or a non-homogeneous temperature distribution in the sample in the axial direction. Thermocouple A was embedded in the center of the snow sample during sample fabrication. As discussed above, the model of Thorpe and Mason [7] suggests that most sublimation occurs in the first few mm of the snow sample. Consequently, it is possible that the snow sample in the region of active sublimation cools more rapidly than our data from probe A indicates. These two possibilities could be tested by additional temperature measurements in the axial direction.

5. The mass-transfer coefficient for snow sublimation

Albert and McGilvary [15] presented a model to calculate sublimation rates directly in an aggregate snow sample. As in [7], the sublimation (or condensation) rate S (kg s^{-1}) in [15] is driven by the difference between the local vapor density (ρ_v) and the saturation vapor density (ρ_{sat}):

$$S = Vh_m a_s(\rho_{sat} - \rho_v) \quad (4)$$

where V is the volume undergoing sublimation, a_s is the specific surface area of snow, and h_m is the mass-transfer coefficient. Since the snow sample radius (7 cm) is larger than that of the air-flow chamber radius (5.25 cm) we use only the portion of the sample undergoing sublimation when calculating V, and use the inner radius of 5.25 cm (see Fig. 1, discussion in Section 2). Because there was no published experimental data on the mass transfer coefficient of snow, the calculations of Albert and McGilvary [15] employed a mass-transfer coefficient for general porous media that was derived for other materials [16]. We now use our data for S, V, v, a_s, and porosity (ϕ), and solve for h_m in each run. In Fig. 5a, we plot our values of h_m from all runs as a function of temperature. The stars in Fig. 5a indicate the value of h_m for each run, assuming sublimation occurs in the first 4 mm of the sample, a mean value suggested by the theory of Thorpe and Mason [7] and consistent with Cahoon et al. [12]; the solid line indicates the best-fit line to these values. The circles indicate the value of h_m assuming sublimation occurs throughout the initial 1 cm of the sample, corresponding to our minimum sample thickness; the thick dashed line indicates the best-fit line to these data. The squares indicate the value of h_m assuming sublimation occurs in the first 1 mm (the minimum value suggested [7] and [12]) the thin dashed line indicates the best-fit line to these data. It is apparent that there is not a strong correlation between h_m and temperature ($r^2 = 0.12$).

In Fig. 5b, we plot our values of h_m from all runs as a function of the modified Reynolds number ($Re = d_p v/v_a(1-\phi)$, where d_p, is the mean particle diameter) as in Albert and McGilvary [15], using the same notation used in Fig. 5a. We find a nearly linear relationship between h_m and the modified Reynolds number ($r^2 = 0.99$), regardless of temperature, suggesting that the modified Reynolds number can be used to reliably calculate h_m for our data. We suggest that the true relationship between h_m and Re lies in the region between the two dashed lines; the solid line is our preferred solution ($h_m = 0.566\ Re + 0.075$), and assumes that sublimation occurs evenly throughout the first 4 mm of the sample thickness, a value supported by [7] and consistent with [12]. We acknowledge that our data cannot provide a unequivocal expression for h_m, but this work significantly improves the relationship of Albert and McGilvary [15] and shows a clear path forward for future revision. We note that it may be possible to further refine this relationship using our results along with lattice Boltzmann methods [17] or mass-transfer calculations based on 3-D microtomography [18] to calculate the actual region of active sublimation in the sample using the measured pore space geometry.

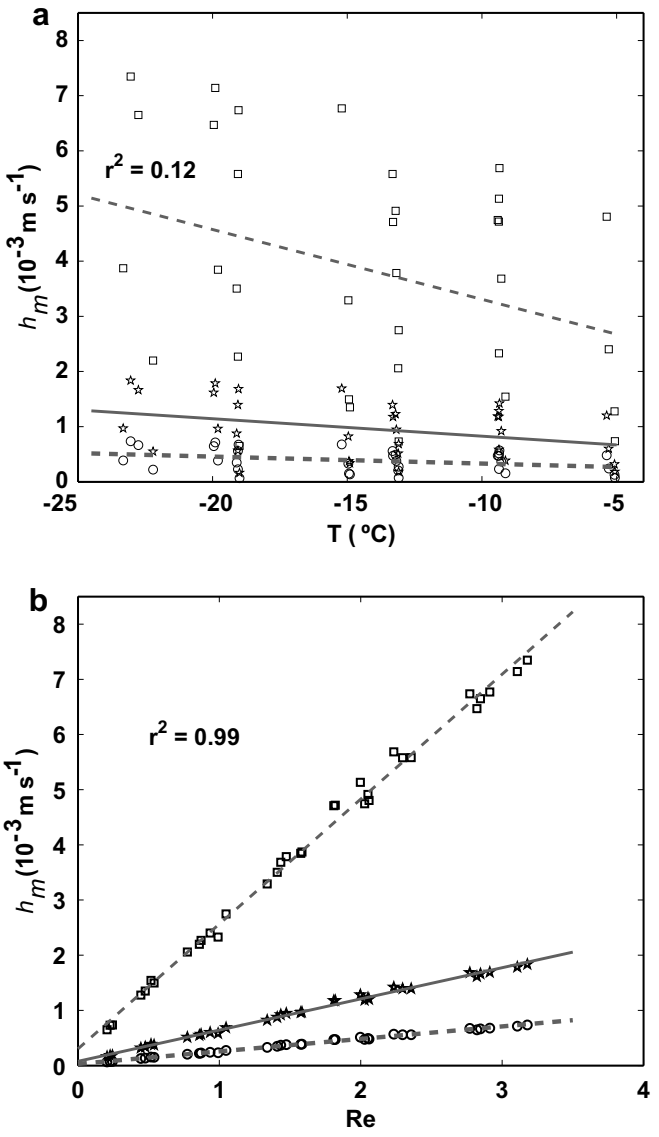

Fig. 5. Mass-transfer coefficient (h_m) as a function of temperature (upper panel) and modified Reynolds number (lower panel). The stars in each panel indicate the value of h_m for each run, assuming sublimation occurs in the first 4 mm of the sample, as suggested by the theory of Thorpe and Mason [7]; the solid line indicates the best-fit line to these values. The circles in each panel indicate the value of h_m assuming sublimation occurs evenly throughout the initial 1 cm of the sample; the thick dashed line indicates a best-fit line to these data. The squares indicate the value of h_m assuming sublimation occurs in the first 1 mm of the sample; the best-fit line is given by the thin dashed line. It is evident that there is only a weak relationship between h_m and temperature ($r^2 = 0.12$), while the relationship with Re is much stronger ($r^2 = 0.99$).

6. Conclusions

We have conducted experiments to determine the sublimation rate of a sieved snow sample between −5 and −23 °C, under forced convection ($0.25 < Re < 3.5$). Our data show that the sublimation rate of snow is very rapid, and that saturation vapor density is reached in the pore spaces within at most the first 1 cm of the snow sample, regardless of temperature or flow rate. These results are broadly consistent with the results of Cahoon et al. [12] and the model presented by Thorpe and Mason [7], although both suggest that saturation could be reached much more quickly. We use the model of Albert and McGilvary [15] to update the formulation of the mass-transfer coefficient, and present a linear relationship between the modified Reynolds number and h_m. We use our data on sublimation rate of snow and assume that the sublimation occurs within the first few mm of the sample to determine the mass-transfer coefficient for snow sublimation as $h_m = 0.566\ Re + 0.075$.

A forthcoming paper will focus on comparing these results with field measurements of snow sublimation [1,19,20]. Additional future work will focus on using the methods outlined above to examine effects of sublimation on stable isotopic ratios.

Acknowledgements

This work was supported by NSF-OPP 0338008 to T. Neumann and NSF-OPP 0337304 to M. Albert. We thank E.J. Steig,

J.S. Wettlaufer and E.D. Waddington for helpful discussions, and an anonymous reviewer for suggestions that have improved the content and clarity of the manuscript.

References

[1] J.E. Box, K. Steffen, Sublimation on the Greenland ice sheet from automated weather station observations, J. Geophys. Res. 106 (D24) (2001) 33965–33981.
[2] S.J. Déry, M.K. Yau, Large-scale mass balance effects of blowing snow and surface sublimation, J. Geophys. Res. 107 (D23) (2002) 4679, doi:10.1029/2001JD001251.
[3] W. Stichler, U. Schotterer, K. Frohlich, P. Ginot, C. Kull, H. Gaggeler, P. Pouyaud, Influence of sublimation on stable isotope records recovered from high-altitude glaciers in the tropical Andes, J. Geophys. Res. 106 (B9) (2001) 22613–22630.
[4] M. Sturm, C. Benson, Vapor transport grain and depth-hoar development in the subarctic snow, J. Glaciol. 43 (143) (1997) 42–59.
[5] I.M. Whillans, P.M. Grootes, Isotopic diffusion in cold snow and firn, J. Geophys. Res. 90 (D2) (1985) 3910–3918.
[6] M.R. Albert, Effects of snow and firn ventilation on sublimation rates, Ann. Glaciol. 35 (2002) 52–56.
[7] A.D. Thorpe, B.J. Mason, The evaporation of ice spheres and ice crystals, Br. J. Appl. Phys. 17 (1966) 541–548.
[8] M. Sakly, G. Lambrinos, Sublimation de la glace sous convection forcee. Determination du coefficient global de transfert de masse, Int. Comm. Heat Mass Transfer 16 (1989) 633–644.
[9] C. Morris, A simple frost-point humidity generator, Meas. Sci. Technol. 8 (5) (1997) 473–478.
[10] J. Tennermann, The chilled mirror dew point hygrometer as a measurement standard, Sensors 16 (1999) 49–54.
[11] W. Wagner, A. Saul, A. Pruss, International equations for the pressure along the melting and along the sublimation curve of the ordinary water substance, J. Phys. Chem. Ref. Data 23 (3) (1994) 515–527.
[12] A. Cahoon, M. Maruyama, J.S. Wettlaufer, Growth-melt asymmetry in crystals and twelve-sided snowflakes, Phys. Rev. Lett. 96 (25) (2006), doi:10.1103/PhysRevLett.96.255502.
[13] W.J. Massman, A review of the molecular diffusivities of H_2O, CO_2, CH_4, CO, O_3, SO_2, NH_3, N_2O, NO, and NO_2 in air, O_2 and N_2 near STP, Atmos. Environ. 32 (6) (1998) 1111–1127.
[14] J. Xiao, R. Bintanja, S.J. Déry, G.W. Mann, P.A. Taylor, An intercomparison among four models of blowing snow, Boundary-Layer Met. 97 (2000) 109–135.
[15] M.R. Albert, W.R. McGilvary, Thermal effects due to air flow and vapor transport in dry snow, J. Glaciol. 38 (129) (1992) 273–281.
[16] J.C. Chu, J. Kalil, W. Wetteroth, Mass transfer in a fluidized bed, Chem. Eng. Prog. 49 (3) (1953) 141–149.
[17] J. Freitag, U. Dobrindt, J. Kipfstuhl, A new method for predicting transport properties of polar firn with respect to gases on the pore-space scale, Ann. Glaciol. 35 (2002) 538–544.
[18] F. Flin, J.-B. Brzoska, The temperature gradient metamorphism: vapor diffusion model and validations using microtomographic images, Ann. Glaciol. 49 (2008) 17–21.
[19] Y. Fujii, K. Kusunoki, The role of sublimation and condensation in the formation of ice sheet surface at Mizuho Station, Antarctica, J. Geophys. Res. 87 (C6) (1982) 4293–4300.
[20] R. Bintanja, M. van den Brooke, The surface energy balance of Antarctic snow and blue ice, J. Appl. Met. 34 (4) (1995) 902–926.